

Article

Adsorption Characteristics of Cetirizine on Graphene Oxide

Tuhin Bhattacharjee^{1,2}, Arnab Bhattacharjee¹, Deepmoni Deka³ , Mihir Kumar Purkait^{3,4,*},
Devasish Chowdhury^{5,*}  and Gitanjali Majumdar^{1,2,*}¹ Department of Chemistry, Assam Engineering College, Guwahati 781013, India² Department of Chemistry, Assam Science and Technology University, Tetelia Road, Jalukbari, Guwahati 781013, India³ Centre for the Environment, Indian Institute of Technology, Guwahati 781039, India⁴ Department of Chemical Engineering, Indian Institute of Technology, Guwahati 781039, India⁵ Material Nanochemistry Laboratory, Physical Science Division, Institute of Advanced Studies in Science and Technology, Paschim Boragaon, Guwahati 781035, India

* Correspondence: mihir@iitg.ac.in (M.K.P.); devasish@iasst.gov.in (D.C.); gitanjalic@gmail.com (G.M.)

Abstract: Water pollution caused by emerging contaminants such as pharmaceutical compounds is a growing problem worldwide. In this reported work, graphene oxide (GO) was directly used to remove an antihistamine drug, cetirizine. GO was prepared from graphite using a modified Hummer's method and was characterized by UV-vis spectroscopy, Fourier-transformed infrared spectroscopy (FTIR), thermogravimetric analyzer (TGA), field scanning electron microscope (FE-SEM), transmission electron microscope (TEM), X-ray diffraction (XRD), etc. GO was demonstrated to be a highly efficient adsorbent for removing cetirizine from an aqueous solution. The adsorption of cetirizine on GO at various pH levels showed that in acidic pH with the adsorption shows faster kinetics and complete removal of cetirizine within 10 min, followed by neutral pH, which showed relatively slower kinetics but complete removal of cetirizine. However, at basic pH, GO could not completely remove cetirizine after 24 h. At a neutral pH, GO showed maximum adsorption of 81.30 mg g⁻¹ of cetirizine. The adsorption isotherm results showed good agreement with the Langmuir isotherm. The BET surface area analysis showed the presence of mesoporosity in GO. In addition, the BET analysis further revealed a type IV isotherm curve being followed. A plausible mechanism is also discussed in the paper. The recyclability experiment demonstrates an adsorption efficiency of 85% after four cycles. The thermodynamic study reveals that adsorption is thermodynamically less favorable at higher temperatures. Hence, the current study successfully demonstrates the use of GO as an efficient adsorbent in removing cetirizine. It also studies the various factors and interactions affecting adsorption. Thus, this study sheds light on the adsorption characteristics of cetirizine on graphene oxide.

Keywords: graphene oxide; cetirizine; adsorption; intraparticle diffusion; BET

Citation: Bhattacharjee, T.; Bhattacharjee, A.; Deka, D.; Purkait, M.K.; Chowdhury, D.; Majumdar, G. Adsorption Characteristics of Cetirizine on Graphene Oxide. *Sustain. Chem.* **2023**, *4*, 209–223. <https://doi.org/10.3390/suschem4020016>

Academic Editors: Valeria La Parola and Leonarda Liotta

Received: 21 February 2023

Revised: 4 April 2023

Accepted: 10 April 2023

Published: 30 May 2023



Copyright: © 2023 by the authors. Licensee MDPI, Basel, Switzerland. This article is an open access article distributed under the terms and conditions of the Creative Commons Attribution (CC BY) license (<https://creativecommons.org/licenses/by/4.0/>).

1. Introduction

Pharmaceutical contamination in different water bodies has attracted attention in recent years due to an alarming overuse and uncontrolled disposal of pharmaceuticals [1]. The industrial discharge of pharmaceuticals has become a rising cause for concern in recent years [2]. Such “Emerging Contaminants” are expected to become a major health hazard in the near future, and increased research efforts are needed for consequent remediation using low-cost sustainable materials [3]. Special attention has to be taken when dealing with emerging pollutants as they generally have complex molecular structures, varied molecular weights, functionalities, and shapes. Moreover, some of the pharmaceuticals are lipophilic and they are moderately soluble in water. Hence, special materials need to be developed to efficiently remove such pollutants from the water.

Cetirizine is one such emerging pollutant belonging to the class of second-generation antihistamine drugs with a piperazine ring, used widely used for the treatment of hay

fever, allergies, angioedema, etc. Unfortunately, more than 80% of cetirizine is excreted due to poor metabolism. Cetirizine is a very stable antihistamine drug, having high solubility, low volatility, lipophilic nature, and low biodegradability. Among the antihistamine drugs, cetirizine is found to have higher potency in the aqueous environment [4]. So, even at ppm levels of cetirizine has been found to exist in various wastewaters, as well as in drinking water [5]. Hence, cetirizine enters aquatic systems in up to micrograms-per-liter quantities and hampers the food chain. It is reported that (2–5) $\mu\text{g ml}^{-1}$ is lethal if found in blood [6]. It causes various side effects such as sleepiness, fatigue, fever, sedation, and blurred vision in humans. Research has shown acute toxicity of antihistamine drugs in children can even lead to death [7].

The uses of cetirizine have been found to have increased tremendously during COVID-19, and hence the ecotoxicological effects are expected to impact all living species in years to come [8]. Hence, the detoxification of the aquatic environment from cetirizine is the need of the hour. Attempts have been made to remove cetirizine via advanced oxidation [9], ultrasound-assisted degradation [10], photocatalytic degradation [11], etc. Until now, to the best of our knowledge, limited research has reported on the adsorption of cetirizine and its derivatives from the aquatic environment. A few research groups have reported the adsorption of cetirizine from aqueous solution using activated carbon and also Ca-modified Montmorillonite [12], etc. GO is reported to be a low-cost adsorbent for a wide range of materials including various types of pharmaceuticals, such as atenolol, diclofenac, ibuprofen, etc. [13]. Thus, Graphene is an innovative adsorbent being explored at present and modifications have been done to increase its efficiency and adsorption capacity. For the removal of cetirizine, a laccase enzyme immobilized GO–alginate composite was reported. However, the roles of laccase and GO were not investigated as adsorption with as-synthesized GO was not tested for the adsorption of cetirizine [14]. Herein, we have reported for the first time the removal of cetirizine with as-synthesized GO, without using any enzyme to observe the role of GO, which is the missing piece of the puzzle in the literature. This has been supplemented using FTIR, XPS, and zeta potential studies which were concluded with a mechanism for the adsorption process.

Since the inception of graphene as a useful 2D material, every known material science group has attempted to use graphene for their specific application first. However, all this hype around graphene was not due to a fluke but rather due to all the advantages it brought to the table, including a high theoretical surface area ($2630 \text{ m}^2 \text{ g}^{-1}$), very high young modulus ($\sim 1.0 \text{ TPa}$), high intrinsic mobility ($200,000 \text{ cm}^2 \text{ v}^{-1} \text{ s}^{-1}$), good optical property and high electrical conductivity [15]. Due to such fascinating properties, graphene was used in various applications such as in conductive films [16], OLED electrodes [17], field effect transistors [18], drug delivery [19], tissue regeneration [20], and environmental remediation [21] to name a few. Graphene is an exceptionally good material for environmental remediation because it has a non-toxic adsorbent with a high theoretical surface area, good porosity, and edge-specific functionality for adsorption. Furthermore, it is easier to functionalize GO with various substituents to improve its efficacy in adsorption [15,22]. Over the years, GO has been investigated for the adsorption of various adsorbents including heavy metals [23], dyes [24], pharmaceuticals [25], personal care products [26], etc.

In light of the emergence of various pharmaceutical pollutants, a large number of efficient adsorbents have been reported over the past few years. These include activated carbon [27], clays [28], metal-organic framework [29,30], covalent-organic framework [31], and biopolymers [32,33]. GO, with its multiple advantages, has been explored for possibilities in aiding the removal of various pharmaceuticals. This is because scaling down the lateral dimension of the graphene sheets increases the surface area, which is expected to enhance the absorption capacity of pharmaceuticals. Recently, Bhattacharjee et al. synthesized beta-cyclodextrin functionalized GO using a solvation-assisted sonochemical process for the removal of atenolol. The functionalized GO was reported to remove a maximum of 52.93 mg g^{-1} of atenolol [25]. In recent years, since COVID-19, many pharmaceuticals are in large demand, especially chloroquine (CQN) and dipyrone (DIP) for treating fever

and other related symptoms. Januário et al. synthesized granular activated carbon from coconut shells and functionalized GO for the removal of CQN and DIP. The adsorbent could remove a maximum of 37.65 mg g^{-1} and 62.43 mg g^{-1} of CQN and DIP, respectively [34]. Mahmoodi et al. synthesized GO with chitosan hydrogel for the removal of diclofenac. The group synthesized GO and amino-functionalized GO to prepare two types of chitosan hydrogels, namely GO2-CTS and AGO2-CTS. Langmuir isotherm results showed maximum removal of 132.11 mg g^{-1} and 129.42 mg g^{-1} in GO2-CTS and AGO2-CTS hydrogel, respectively [35].

In this work, we demonstrated GO as an efficient adsorbent in the removal of cetirizine from an aqueous solution with very high efficiency. We have analyzed the adsorption process using various parameters including kinetics, thermodynamic, and diffusion processes. The maximum adsorption capacity of cetirizine in GO was evaluated. The possible experimental evidence for various interactions between GO and cetirizine was evaluated using FTIR and zeta potential. Overall, the goal of this work is to study the adsorption characteristics of GO regarding antihistamine drugs such as cetirizine. This will allow researchers to systematically modify adsorbents for higher efficiency, especially antihistamine drugs such as cetirizine.

2. Materials and Methods

2.1. Materials

Graphite powder, reagent grade sulfuric acid, hydrogen peroxide, and potassium permanganate were supplied from Merck, India. Cetirizine (Cadila) was procured commercially from a local pharmaceutical store. Double-distilled water was used as a solvent.

2.2. Synthesis of GO

GO for the adsorption experiment was prepared using a modified Hummer's method with few modifications [25]. In total, 3 g of graphite powder was mixed with 46 mL of sulfuric acid in a 500 mL beaker with constant stirring in an ice bath below 5°C . Slowly, 9 g of potassium permanganate was added to the mix under constant stirring at $0^\circ\text{--}5^\circ\text{C}$ for 2 h. Subsequently, 150 mL of distilled water was poured under vigorous stirring followed by the addition of 15 mL of hydrogen peroxide, which resulted in the formation of a yellow slurry. The slurry was left undisturbed overnight, and the resulting mixture was washed continuously with double-distilled water until reaching pH 6. The obtained mixture was dried in an oven to obtain a dark brownish powder.

2.3. Preparation of Cetirizine Solutions

In total, 25 mg of a commercially procured cetirizine tablet was dissolved in a 250 mL volumetric flask (99.75 mg L^{-1}). Then, 23.15 mL of the same solution was taken and made up to 100 mL in a volumetric flask to obtain 23.09 mg L^{-1} cetirizine. For adsorption isotherm experiments, 3 tablets with 25 mg of cetirizine dissolved in 250 mL water were used to obtain a 300 mg L^{-1} cetirizine solution.

2.4. Contact Time Experiment, Kinetics, and Diffusion Studies

About 0.01 g of GO was weighed followed by the addition of 10 mL cetirizine of known concentration (23.09 mg L^{-1}) in a 25 mL beaker. The UV-vis spectrophotometer was used to monitor the adsorption of cetirizine with time. Cetirizine showed a characteristic peak at 232 nm, which was used to monitor the presence of cetirizine in an aqueous solution. The scheme of the overall experiment is given in Figure 1.

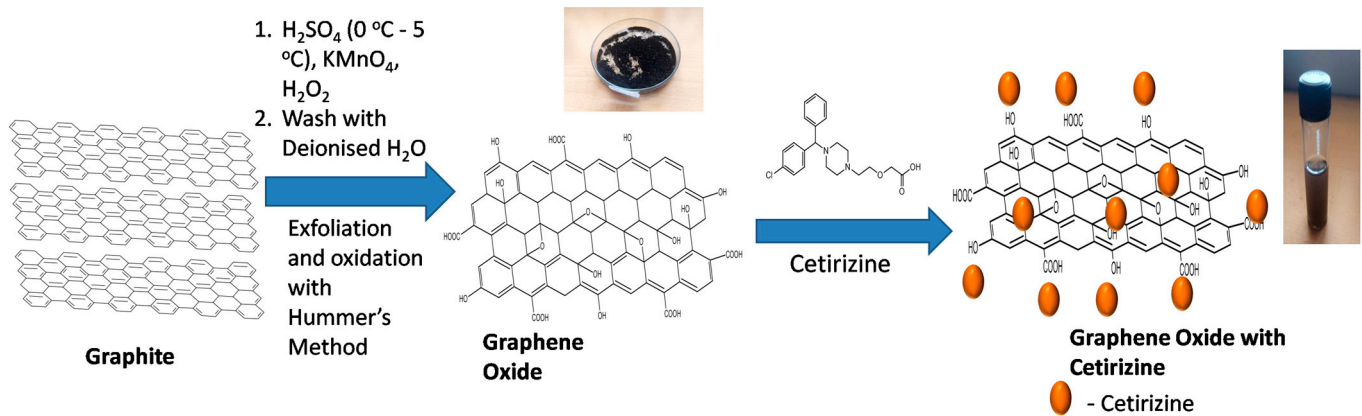


Figure 1. Scheme of preparation of GO and adsorption of cetirizine.

The kinetics of the adsorption process of cetirizine with GO were performed for 23.09 mg L^{-1} cetirizine over 24 h at a neutral pH. Pseudo-first-order (Equation (1)) [36] and pseudo-second-order (Equation (2)) [36] kinetics formulae were employed by linearly fitting the data obtained experimentally. The formulae for pseudo-first-order and second-order are stated below:

$$\ln(q_e - q_t) = -k_1 t + \ln(q_e) \quad (1)$$

$$t/q_t = t/q_e + 1/k_2 q_e^2 \quad (2)$$

where q_e (mg g^{-1}) and q_t (mg g^{-1}) are the amount of cetirizine adsorbed at equilibrium and at any course in time ' t ' (min), respectively. k_1 (min^{-1}) and k_2 ($\text{g mg}^{-1} \text{ min}^{-1}$) are the pseudo-first-order and pseudo-second-order rate constants, respectively.

The most widely accepted intraparticle diffusion model is given by Weber and Morris (1963) [37] (Equation (3)):

$$q_t = k_i t^{1/2} + C \quad (3)$$

From the above equation, it can be stated that intraparticle diffusion is a rate-limiting step in the adsorption process, where the plot of q_t vs. $t^{1/2}$ yields a straight line. k_i is the intraparticle diffusion rate constant $\text{g mg}^{-1} \text{ min}^{-1}$ and C is the surface adsorption. The plot gives a straight line that passes through the origin, which signifies that intra-particle diffusion plays a vital role in the diffusion process. However, a straight line does not pass through the origin, indicating that boundary layer diffusion also takes place in the adsorption process. Thus, the greater the value of C , the greater the contribution of the boundary layer in the diffusion process.

2.5. Effect of pH

To monitor the effect of pH on the adsorption of cetirizine by GO in various conditions, three cetirizine solutions at pH 4, 6, and 10 were prepared to signify acidic, neutral, and basic conditions, respectively. To prepare the solutions of 23.09 mg L^{-1} cetirizine at various pH levels, first, a cetirizine tablet was dissolved in pH 4, 6, and 10 solutions. About 23.15 mL of cetirizine was taken from the stock solution, and the volume was made up to 100 mL with the required pH solution (pH 4, 6, and 10) to obtain a pH-specific 23.09 mg L^{-1} cetirizine solution.

In the adsorption process, 0.01 g of GO was added to 10 mL of cetirizine of specific pH. The adsorption process was monitored at different intervals using a UV-vis spectrophotometer.

2.6. Thermodynamic Studies

The effect of temperature on the adsorption of cetirizine in GO was studied at three different temperatures, namely 298.15 K, 313.15 K, and 333.15 K. With due consideration of exchange adsorption, the value of k° is calculated as follows [38]:

$$k^{\circ} = 55.5 (k_p M_{\text{adsorbate}}) \quad (4)$$

where k_p is the equilibrium constant at time t (L g^{-1}), $M_{\text{adsorbate}}$ is the molecular weight of cetirizine, and 55.5 is the molar concentration of water.

ΔG° was calculated from the equation

$$\Delta G^{\circ} = -RT \ln(k^{\circ}) \quad (5)$$

where T is the temperature in Kelvin, and R is the gas constant ($8.314 \text{ J K}^{-1} \text{ mol}^{-1}$).

Thermodynamic parameters such enthalpy (ΔH°) and entropy (ΔS°) can be calculated from the equation [38]

$$\Delta G = \Delta H^{\circ} + T\Delta S^{\circ} \quad (6)$$

The plot of $\ln(k^{\circ})$ vs. $1/T$ gives a straight line. The slope and intercept of this straight line are used for the determination of ΔH° and ΔS° , respectively.

The negative value of ΔG° indicated the spontaneity or feasibility of the adsorption process. A positive value of ΔS° indicated increased disorder at the solid–liquid interface. A positive ΔH° indicates an exothermic, while a negative ΔH° indicates an endothermic process.

2.7. Adsorption Isotherm Studies

The maximum adsorption capacity of cetirizine with GO was measured. The Langmuir and Freundlich isotherms were obtained by taking seven sets of different concentrations of cetirizine (4.62 mg L^{-1} , 23.09 mg L^{-1} , 46.18 mg L^{-1} , 69.27 mg L^{-1} , 92.36 mg L^{-1} , 138.54 mg L^{-1} and 230.91 mg L^{-1}). Then, 0.01 g of adsorbent was added to each set of cetirizine solutions of 20 mL and kept for 24 h to obtain equilibrium in the adsorption process. The experimental data were fit linearly to obtain both Langmuir [39] and Freundlich [25,39] isotherms, respectively, as given in the formulae below.

$$C_e/Q_e = C_e/Q_m + 1/Q_m k_L \quad (7)$$

$$\ln Q_e = \ln(k_F) + (1/n) \ln(C_e) \quad (8)$$

where q_m (mg g^{-1}) is the maximum uptake of cetirizine, k_L (L mg^{-1}) is the Langmuir adsorption equilibrium constant, and k_F (L mg^{-1}) is the Freundlich constant representing the adsorption capacity. n is a dimensionless constant.

Q_e is calculated using the equation (Equation (6)) below

$$Q_e = (C_o - C_e)V/m \quad (9)$$

where V is the volume of the cetirizine solution taken in a liter, m is the mass of GO in g, C_o is the initial concentration (mg L^{-1}) of the cetirizine before adsorption, and C_e is the equilibrium concentration (mg L^{-1}) of the adsorbate.

2.8. Recyclability

Recyclability is an important parameter for adsorption to be sustainable. To check the recyclability, the cetirizine present in GO must be removed. In our case, we have used two methods of removing cetirizine from GO. In one process, we regenerated the adsorbent by adding 50 μL of H_2O_2 in 10 mL of water. This will degrade the cetirizine present in

graphene oxide. In the other process, because of the known solubility of cetirizine in DMSO, it was used as a solvent to desorb cetirizine from GO.

2.9. Characterization Techniques of Adsorbent

The layered structure of GO was investigated using a transmission electron microscope (TEM) from Jeol 2100 Plus, Japan. The different functional groups in the 500–4000 cm^{-1} range in GO and cetirizine adsorbed in GO were investigated in attenuated total reflection (ATR) mode using a Spectrum Series, Perkin Elmer FTIR instrument. The XRD spectrum of the GO powder was taken using a Bruker D8 Advance diffractometer, with Cu radiation operating at 40 kV and 40 mA. The zeta potential was taken for both GO and GO–cetirizine Melvern ZS90. The UV–visible spectrum of GO was characterized using a UV–Vis Spectrophotometer (LABTRONICS MODEL LT-2201). In addition, all the adsorption experiments of cetirizine in GO were evaluated using the same UV–vis spectrophotometer model. The BET analysis was performed using a Micrometrics Tristar II 3020 model, where N_2 gas was purged into the sample. The BET conditions are stated in a Table S1 in the Supplementary Materials.

3. Results and Discussion

3.1. Characterization of GO

As stated earlier, the GO was prepared from graphite using a modified Hummer's method. The UV–visible spectrum of GO is shown in Figure 2A. The UV–visible spectrum shows a peak at 234 nm. The peak corresponds to π – π^* transition in the fused conjugated benzene-like moieties present in GO [40]. The FTIR spectrum of GO was also carried out (Figure 2B) and the FTIR of GO exhibits major peaks at 3200 cm^{-1} (broadened peak), 1619 cm^{-1} , 1397 cm^{-1} , and 1049 cm^{-1} because of O–H stretching with H-bonding, C=C stretching of aromatic C=C, C–H/C–O–H bending vibrations, and C–O–C stretching vibrations of GO, respectively. The minor peaks 1721 cm^{-1} and 976 cm^{-1} were due to the C=O stretching of the carboxylic acid and the bending of the alkene. The surface charge analysis for GO was performed using a zeta potential analyzer, as shown in Figure 2C. The surface charge of GO was found to be -40.74 mV, which can be attributed to the presence of negatively charged species such as carboxylic acid and a hydroxyl group in GO. The structural order of GO was scrutinized using an X-ray diffractometer in Figure 2D. The GO shows a 2θ peak at 11.08° corresponding to the (0 0 1) crystal plane [40]. The nanosheet-like structure of GO was investigated using a transmission electron microscope (TEM) and is illustrated in Figure 2E. The TEM image shows multiple layered sheets of GO stacked above one another.

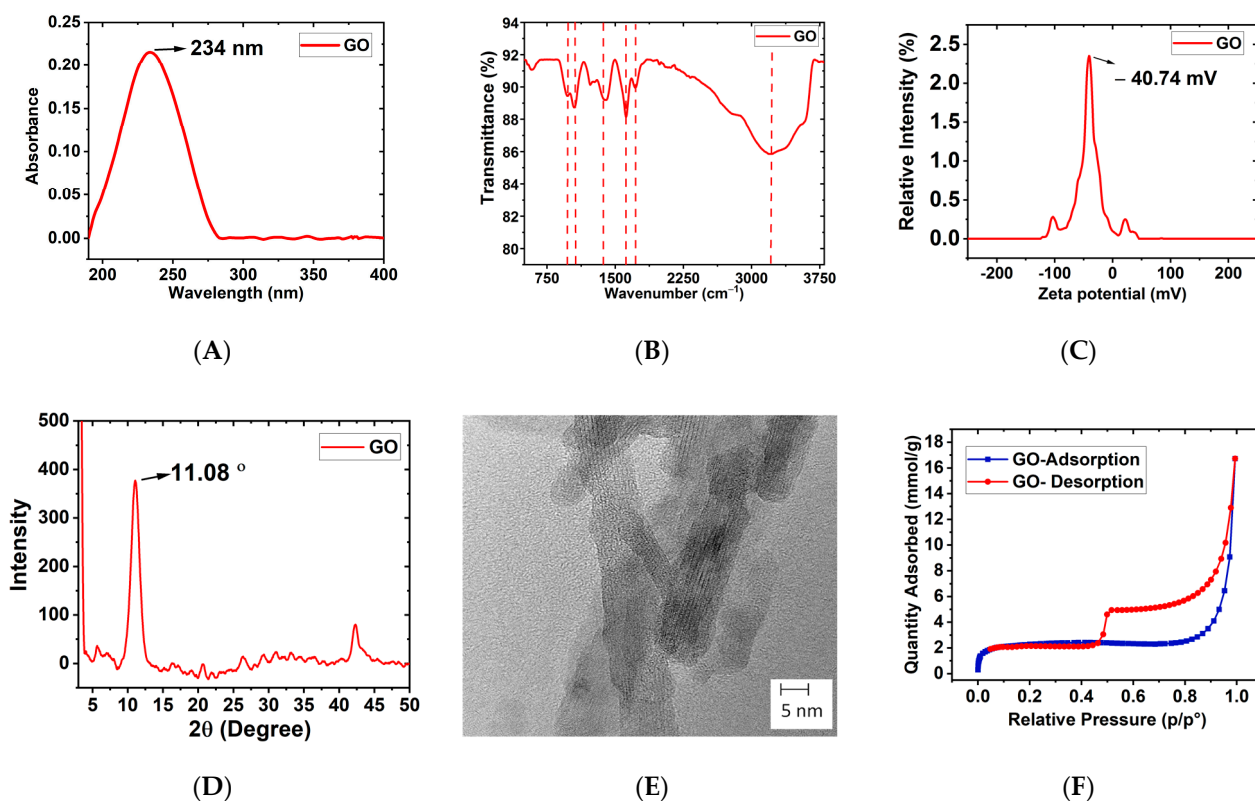


Figure 2. (A) UV–visible spectra, (B) FTIR, (C) zeta, (D) XRD, and (E) TEM and (F) BET of GO.

The BET isotherm is particularly helpful in indicating the adsorption process in the adsorbent, especially in case there is the formation of a multilayer. The BET isotherm of GO shows a resemblance to a BET type IV curve shown in Figure 2F. The sharp knee at the beginning of the isotherm indicates the formation of a monolayer, as predicted by the Langmuir isotherm. When the relative pressure is near unity, there is a sharp increase in the adsorption of N_2 which is probably due to the multilayer formation and bulk liquefaction of N_2 [41]. The surface area and pore size of GO were found to be $11.13 \text{ m}^2 \text{ g}^{-1}$ and 8.82 nm , respectively.

3.2. Contact Time Experiment, Kinetics, and Diffusion Studies

The contact time experiment for the adsorption of cetirizine on GO showed ultra-fast removal of cetirizine, with 99.62% removed within 30 min. Even after 24 h, there was no desorption of cetirizine in the solution. The cetirizine left in solution (%) with time is shown in Figure 3A. The experiment demonstrates the effective adsorption of cetirizine by GO.

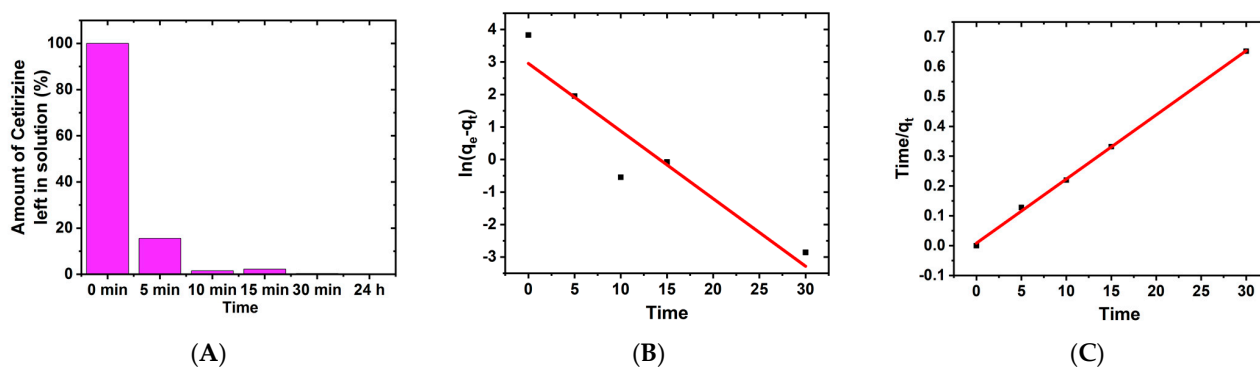


Figure 3. (A) Contact Time experiment of GO with 23.09 mg L^{-1} cetirizine at 298.15 K . (B) Pseudo-first-order and (C) Pseudo-second-order kinetics plots of the cetirizine adsorption experiment.

The pseudo-first and second-order kinetics were also studied [Figure 3B, C]. K_1 and K_2 values for pseudo-first order and pseudo-second-order were found to be 0.208 min^{-1} and $0.055 \text{ g mg}^{-1} \text{ min}^{-1}$, respectively. It is however to be noted that the experiment showed good agreement with pseudo-second order kinetics, with R^2 being 0.999. The kinetics study points to the fact that adsorption follows pseudo-second order kinetics. The results of the pseudo kinetics experiments are given in Table 1.

Table 1. Pseudo kinetics data of adsorption of cetirizine on GO.

Sl. No	Pseudo 1st Order	Pseudo 2nd Order
1.	$K_1 = 0.208 \text{ min}^{-1}$	$K_2 = 0.055 \text{ g mg}^{-1} \text{ min}^{-1}$
2.	$q_e = 19.220 \text{ mg g}^{-1}$	$q_e = 46.490 \text{ mg g}^{-1}$
3.	$R^2 = 0.885$	$R^2 = 0.999$

From the plot in Figure 4, a straight line was observed, which, however, does not pass through the origin. For the adsorption of cetirizine and GO, K_i and C were found to be $1.083 \text{ g mg}^{-1} \text{ min}^{-1}$ and 15.218, respectively. The non-zero value of constant C indicates that other than intraparticle diffusion, there exists diffusion of the boundary layer along with other processes, leading to the adsorption of cetirizine into the pores of GO. Thus, the boundary layer and other processes play a vital role in the adsorption process [42–44].

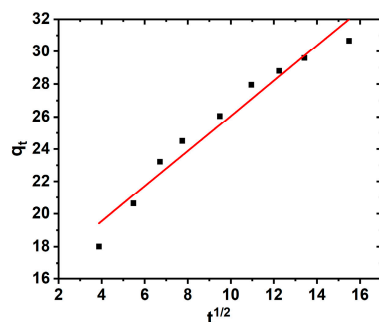


Figure 4. Intraparticle Diffusion model plot q_t vs. $t^{1/2}$.

3.3. pH Variation Studies

One of the most interesting facets of the experiment was the dependence of pH (Figure 5) on the adsorption process. It was found that at pH 4 and 6, being acidic and neutral pH, respectively, there was ultrafast removal, and over 99% of cetirizine could be removed within the first 30 min. However, in basic pH, the adsorption process became quite sluggish, and only 58.86% of cetirizine could be removed after 120 min. Overall, in basic conditions, GO could not remove cetirizine even after 24 h, with only 86.61% removal. The rate of adsorption of cetirizine (mg L^{-1}) at different pH levels is shown in Figure 5.

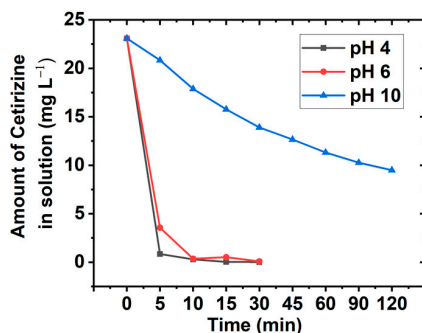


Figure 5. pH variation studies of adsorption of cetirizine in GO.

3.4. Thermodynamics Studies

The adsorption plot in Figure 6A of GO with cetirizine results in a non-linear plot, and it was observed that the higher the temperature, the lower the adsorption of cetirizine. It is possible that the bonding of GO with cetirizine is due to the formation of hydrogen bonding with different functional moieties in cetirizine and GO. As such bonding is weak, at a higher temperature, molecules have higher energy and a lesser tendency to form H-bonding with GO. This leads to lower adsorption at higher temperatures, as observed in Figure 6A.

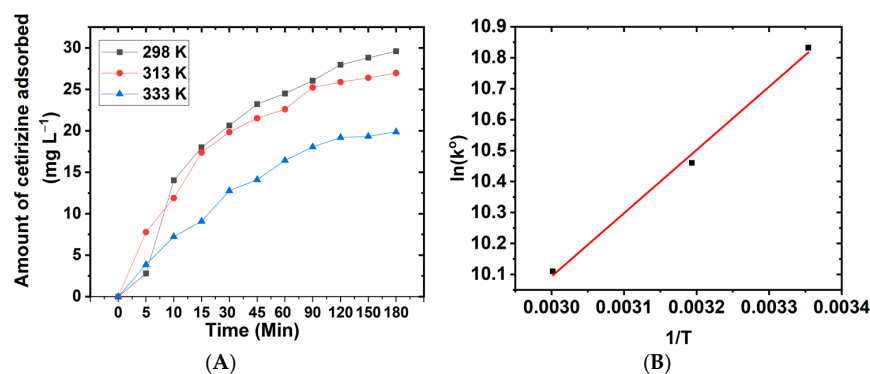


Figure 6. (A) Thermodynamics plot of adsorption of cetirizine on GO and (B) $\ln(k^0)$ vs. T^{-1} .

The values of ΔH° , ΔS° , and ΔG° are depicted in Table 2 below after calculation from $\ln(k^0)$ vs. T^{-1} plot in Figure 6B. As ΔG° is negative, it can be concluded that the adsorption process is spontaneous and thermodynamically feasible. As observed from the data for enthalpy, the adsorption of cetirizine on GO is exothermic, and weak bonds such as H-bonds play a vital role in the adsorption process.

Table 2. Calculation of the Thermodynamic Parameters.

Sl. No	Temperature (K)	ΔG° (KJ mol ⁻¹)	ΔH° (KJ mol ⁻¹)	ΔS° (J K ⁻¹ mol ⁻¹)
1.	298.150	-26.852		
2.	313.150	-27.234	-16.984	33.000
3.	333.150	-28.002		

3.5. Langmuir and Freundlich Isotherm

The adsorption isotherms help in predicting the mechanism of the adsorption process. The Langmuir process helps us to predict single molecular layer adsorption, while the Freundlich process predicts the formation of a multilayer during the adsorption process. The isotherm studies were carried out via batch experiments with concentrations of 4.62 mg L⁻¹, 23.09 mg L⁻¹, 46.18 mg L⁻¹, 69.27 mg L⁻¹, 92.36 mg L⁻¹, 138.54 mg L⁻¹, and 230.91 mg L⁻¹. The R² shows good agreement with the Langmuir isotherm, suggesting monolayer formation after adsorption. The Langmuir and Freundlich rate constants and other related isotherm data have been given in Table 3. The Langmuir and Freundlich isotherms are shown in Figure 7A,B, respectively.

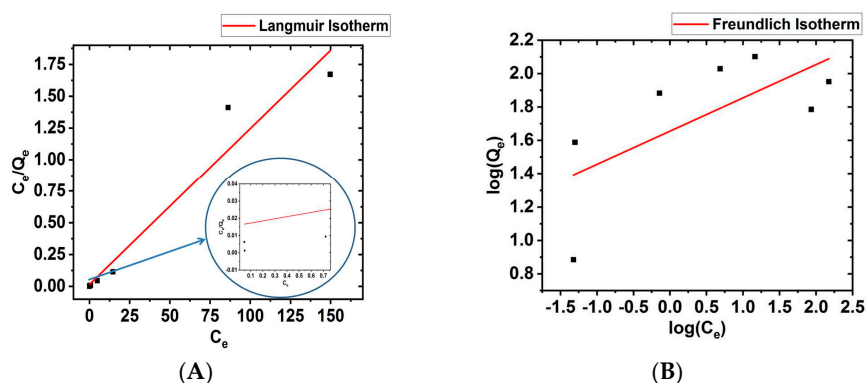


Figure 7. Isotherm studies of GO: (A) Langmuir and (B) Freundlich isotherm.

Table 3. Isotherm data related to adsorption of cetirizine on GO.

Sl. No	Langmuir Isotherm	Freundlich Isotherm
1.	$K_L = 0.766 \text{ L mg}^{-1}$	$K_F = 5.014 \text{ L mg}^{-1}$
2.	$q_M = 81.300 \text{ mg g}^{-1}$	$n = 5.235$

3.6. XPS Analysis

The surface functional moieties present in GO after cetirizine adsorption were determined using X-ray photoelectron spectroscopy and depicted in Figure 8. From our previous report, the spectral analysis of GO for C1s spectra showed peaks at 284.73 eV, 286.71 eV, and 287.75 eV corresponding to C–C, C–OH, and C=O, respectively, while in O1s spectra (Figure 8B), peaks 531.1 eV, 532.56 eV, and 533.4 eV corresponded to –COOH, C=O, and C–OH, respectively [25]. After the adsorption of cetirizine, C1s peaks corresponding to C–C, C–O, and C=O were present at 284.67 eV, 286.73 eV, and 287.86 eV, respectively (Figure 8B). As for O1s spectra after adsorption, peaks were observed at 532.33 eV and 533.87 eV, which are related to C=O and C–OH, respectively (Figure 8C) [25].

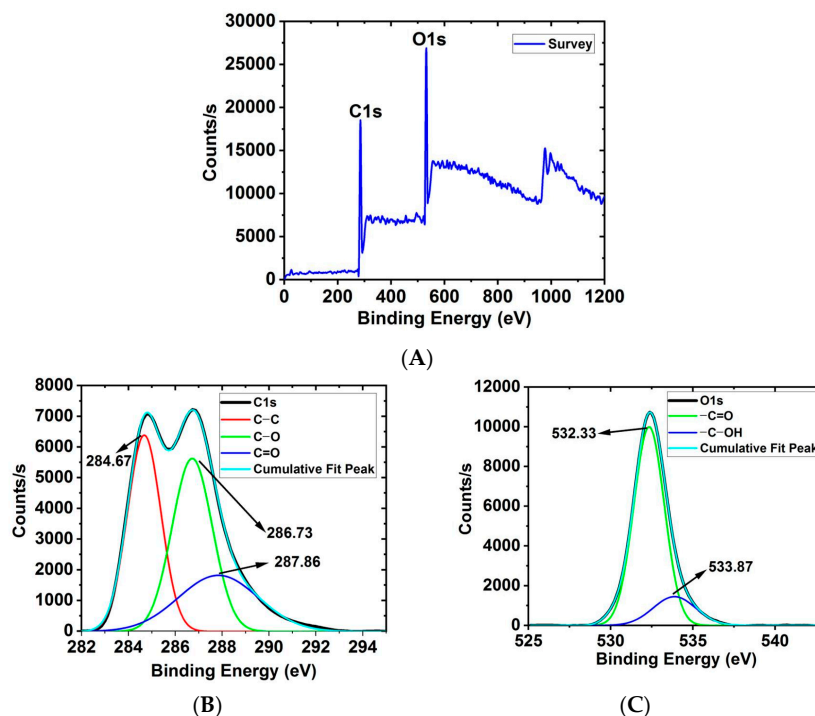


Figure 8. XPS (A) survey, (B) C1s and (C) O1s spectra of GO–cetirizine.

3.7. Recyclability

After four cycles of adsorption of cetirizine on GO (Figure 9), it was observed that 85% efficiency in adsorption was retained in DMSO-treated GO, while in H_2O_2 , the adsorption efficiency of 68% was retained. Hence, desorption using DMSO is better than the peroxide-treated GO–cetirizine system. It is also visible that adsorption efficiency decreases in the subsequent cycle. This could be because complete regeneration of the surface site is not achieved during desorption using DMSO and H_2O_2 .

The structural stability of the GO after four cycles of adsorption of cetirizine on GO was checked using a scanning electron microscope (SEM) image, and the microstructure was compared with as-synthesized GO. The representative SEM image of as-synthesized GO is shown in Figure S1A, Supplementary Materials. The representative SEM of GO after four cycles of adsorption of cetirizine and subsequent desorption with H_2O_2 and representative SEM of GO after four cycles of adsorption of cetirizine and subsequent desorption with DMSO are shown in Figure S2B,C, respectively (Supplementary Materials). It is evident from the SEM images that even after four cycles and desorption with H_2O_2 and DMSO, the structural features of GO are intact; however, some debris is visible over the graphene sheet.

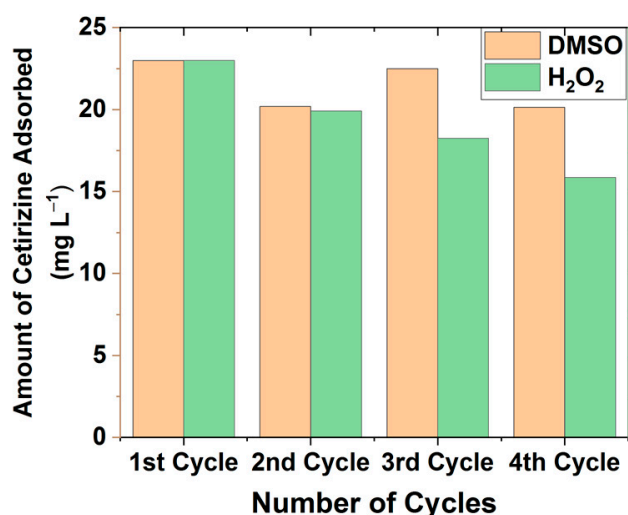


Figure 9. Recyclability experiment of GO.

3.8. Mechanism

To decipher the mechanistic process of the adsorption of cetirizine in GO, FTIR, and zeta potential analyses were taken into consideration. The FTIR spectrum gave information about various covalent interactions, while the zeta potential showed the presence of any electrostatic interactions. The findings from the FTIR and zeta potential analyses of GO are mentioned in the previous discussion.

From the FTIR spectrum of cetirizine, it was observed that cetirizine had major peaks at 1058 cm^{-1} , 1406 cm^{-1} , 1629 cm^{-1} , and 3196 cm^{-1} resulting from C–O–C stretching vibrations, C–H bending vibrations, C=C of benzene of cetirizine, and N–H (amine)/C–OH (carboxylic acid) stretching frequencies, with H-bonding broadening in cetirizine. Other minor peaks including 984 cm^{-1} , 1235 cm^{-1} , and 1731 cm^{-1} were due to bending stretching of the alkene, C–N stretching of the amine, and C=O stretching of the carboxylic acid (Figure 10A). After the adsorption of cetirizine on GO, the peaks observed were mostly similar to cetirizine but with some peaks having an increase in intensity due to similar groups being present in both cetirizine and GO. The peak at 3204 cm^{-1} was due to O–H stretching from both GO and also the N–H stretching of cetirizine. The peak was sharpened compared to GO and cetirizine, suggesting a decrease in H-bonding, possibly due to the presence of other types of interactions between GO and cetirizine. The sharp peak at

1620 cm^{-1} was due to the aromatic C=C of GO and C=C of the benzene ring of cetirizine (Figure 10A). π - π stacking is also possible between an aromatic system of GO and the benzene ring of cetirizine [45]. The C-H bending vibrations of methyl/methylene groups in cetirizine and GO, as well as C-O-H bending vibrations in cetirizine (carboxylic acid) and GO (alcoholic/carboxylic acid) resulted in a sharp peak at 1397 cm^{-1} .

Furthermore, in zeta analysis (Figure 10B), there was also a decrement in zeta potential from -40.74 mV to -35.78 mV in GO-cetirizine. This can be attributed to electrostatic interaction possibly between two protonated tertiary amines in cetirizine with negatively charged groups (carboxylic acids/hydroxyl groups) in GO. Such interaction may lead to a decrease in H-bonding. The mechanism with various bonding interactions is highlighted in Figure 10C. The zeta potential interaction at different pH is discussed in the Supplementary Material (Figure S1).

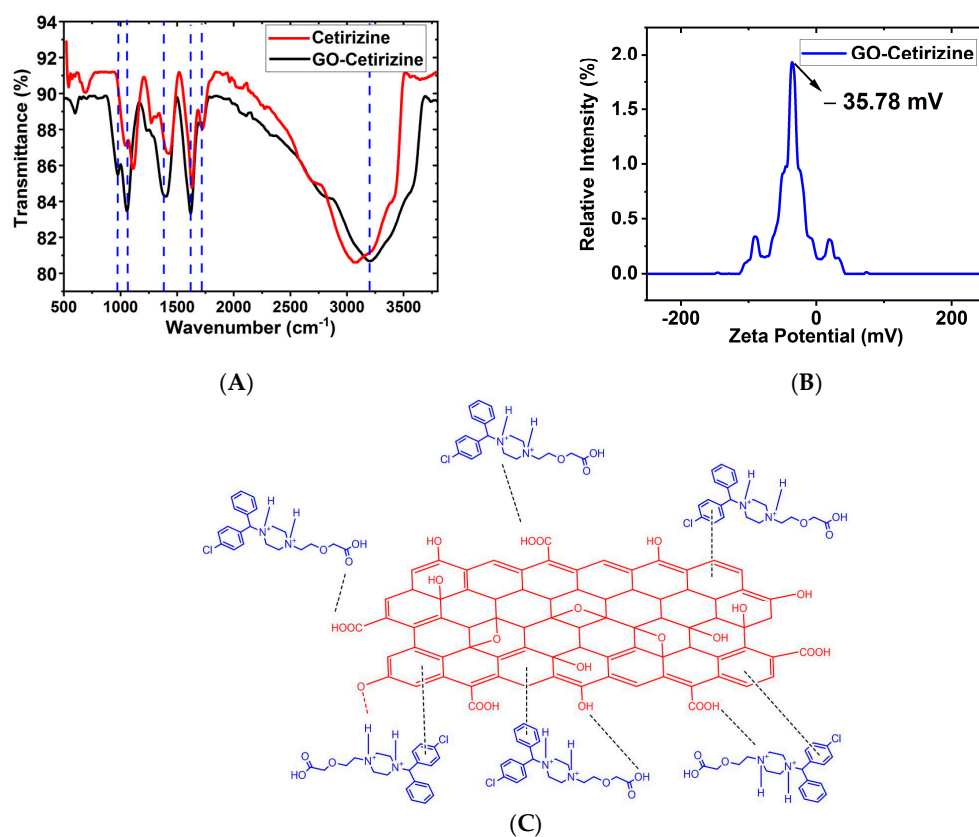


Figure 10. (A) FTIR and (B) zeta of GO-cetirizine. (C) Mechanism of adsorption of cetirizine on GO.

4. Conclusions

In summary, we have synthesized GO from graphite using a modified Hummer's method. The GO synthesized was confirmed using TEM, XRD, and UV-visible spectroscopy, etc. Cetirizine was taken as the model for an antihistamine drug for adsorption on GO. The adsorption process showed fast removal of cetirizine within 30 min in acidic and neutral conditions. The removal of cetirizine was found to be a maximum of 81.30 mg g^{-1} . After analysis with FTIR and zeta, it can be concluded that π - π interactions, H-bonding, as well as electrostatic interactions played a role in the binding of cetirizine with GO. Such interactions are found to be pH-dependent. The BET analysis exhibited the presence of mesopores that are highly likely to assist in the adsorption process. Hence, the overall process is highly efficient and cost-effective. Such systems can be further employed for the removal of other pharmaceutical drugs that are accumulating in the environment, especially during the post-COVID-19 situation.

Supplementary Materials: The following supporting information can be downloaded at <https://www.mdpi.com/article/10.3390/suschem4020016/s1>, Table S1: BET condition of GO; Figure S1: Zeta potential of Cetirizine in acidic pH, Zeta potential of GO-Cetirizine in acidic pH, Zeta potential of Cetirizine in basic pH and Zeta potential of GO-Cetirizine in basic pH. SEM image of as-synthesized GO, used four times in the adsorption of Cetirizine and subsequent desorption with H₂O₂ and DMSO. Figure S2: Representative Scanning Electron Microscope (SEM) of as synthesized GO, Representative Scanning Electron Microscope (SEM) of GO after using four times in adsorption of Cetirizine and subsequent desorption with H₂O₂, Representative Scanning Electron Microscope (SEM) of GO after using four times in adsorption of Cetirizine and subsequent desorption with DMSO.

Author Contributions: Conceptualization, T.B. and G.M.; formal analysis, T.B. and G.M.; investigation, T.B., G.M., A.B., D.D.; writing—original draft preparation, T.B., G.M., M.K.P., D.C.; writing—review and editing, T.B., G.M., M.K.P., D.C.; supervision, G.M., M.K.P., D.C.; Funding acquisition, G.M. All authors have read and agreed to the published version of the manuscript.

Funding: This research was funded by Assam Science Technology and Environment Council (ASTEC), grant number ASTEC/S&T/1802/1/2019-20/1574-1588 and Centre for Education Technology, IIT Guwahati, grant number IITG/CET/TEQIP-III/CR/2020-21/04.

Institutional Review Board Statement: Not applicable.

Informed Consent Statement: Not applicable.

Data Availability Statement: The data presented in this study are available on request.

Acknowledgments: We would like to thank Central Instrumentation Facility (CIF) IIT Guwahati, and SAIC-IASST for their instrumental support. We especially thank Sazzadur Rahman for his help with the research.

Conflicts of Interest: The authors declare no conflict of interest.

References

1. Patel, M.; Kumar, R.; Kishor, K.; Mlsna, T.; Pittman, C.U.; Mohan, D. Pharmaceuticals of Emerging Concern in Aquatic Systems: Chemistry, Occurrence, Effects, and Removal Methods. *Chem. Rev.* **2019**, *119*, 3510–3673. [[CrossRef](#)]
2. Larsson, D.G.J.; de Pedro, C.; Paxeus, N. Effluent from Drug Manufactures Contains Extremely High Levels of Pharmaceuticals. *J. Hazard. Mater.* **2007**, *148*, 751–755. [[CrossRef](#)]
3. Valdez-Carrillo, M.; Abrell, L.; Ramírez-Hernández, J.; Reyes-López, J.A.; Carreón-Díazconti, C. Pharmaceuticals as Emerging Contaminants in the Aquatic Environment of Latin America: A Review. *Environ. Sci. Pollut. Res.* **2020**, *27*, 44863–44891. [[CrossRef](#)] [[PubMed](#)]
4. Majumder, J.; Deb, J.; Husain, A.; Jana, S.S.; Dastidar, P. Cetirizine Derived Supramolecular Topical Gel in Action: Rational Design, Characterization and in Vivo Self-Delivery Application in Treating Skin Allergy in Mice. *J. Mater. Chem. B* **2015**, *3*, 6634–6644. [[CrossRef](#)] [[PubMed](#)]
5. Fick, J.; Söderström, H.; Lindberg, R.H.; Phan, C.; Tysklind, M.; Larsson, D.G.J. Contamination of surface, ground, and drinking water from pharmaceutical production. *Environ. Toxicol. Chem.* **2009**, *28*, 2522. [[CrossRef](#)] [[PubMed](#)]
6. Schulz, M.; Schmoldt, A. Therapeutic and toxic blood concentrations of more than 800 drugs and other xenobiotics. *Pharmazie* **2003**, *58*, 447–474.
7. Reyes-Jacang, A.; Wenzl, J.E. Antihistamine Toxicity in Children. *Clin. Pediatr. Phila.* **1969**, *8*, 297–299. [[CrossRef](#)]
8. May, B.C.; Gallivan, K.H. Levocetirizine and Montelukast in the COVID-19 Treatment Paradigm. *Int. Immunopharmacol.* **2022**, *103*, 108412. [[CrossRef](#)]
9. He, X.; O'Shea, K.E. Rapid Transformation of H1-Antihistamines Cetirizine (CET) and Diphenhydramine (DPH) by Direct Peroxymonosulfate (PMS) Oxidation. *J. Hazard. Mater.* **2020**, *398*, 123219. [[CrossRef](#)]
10. Sutar, R.S.; Rathod, V.K. Ultrasound Assisted Enzyme Catalyzed Degradation of Cetirizine Dihydrochloride. *Ultrason. Sonochem.* **2015**, *24*, 80–86. [[CrossRef](#)]
11. Uheida, A.; Mohamed, A.; Belaqziz, M.; Nasser, W.S. Photocatalytic Degradation of Ibuprofen, Naproxen, and Cetirizine Using PAN-MWCNT Nanofibers Crosslinked TiO₂-NH₂ Nanoparticles under Visible Light Irradiation. *Sep. Purif. Technol.* **2019**, *212*, 110–118. [[CrossRef](#)]
12. Li, Z.; Chang, P.-H.; Jean, J.-S.; Jiang, W.-T.; Hong, H. Mechanism of Chlorpheniramine Adsorption on Ca-Montmorillonite. *Colloids Surf. A Physicochem. Eng. Asp.* **2011**, *385*, 213–218. [[CrossRef](#)]
13. Khan, A.; Wang, J.; Li, J.; Wang, X.; Chen, Z.; Alsaedi, A.; Hayat, T.; Chen, Y.; Wang, X. The Role of GO and GO-Based Nanomaterials in the Removal of Pharmaceuticals from Aqueous Media: A Review. *Environ. Sci. Pollut. Res.* **2017**, *24*, 7938–7958. [[CrossRef](#)] [[PubMed](#)]

14. Sharifi-Bonab, M.; Arjomandi Rad, F.; Talat Mehrabad, J. Preparation of Laccase-GO Nanosheet/Alginate Composite: Application for the Removal of Cetirizine from Aqueous Solution. *J. Environ. Chem. Eng.* **2016**, *4*, 3013–3020. [[CrossRef](#)]
15. Zhu, Y.; Murali, S.; Cai, W.; Li, X.; Suk, J.W.; Potts, J.R.; Ruoff, R.S. Graphene and GO: Synthesis, Properties, and Applications. *Adv. Mater.* **2010**, *22*, 3906–3924. [[CrossRef](#)]
16. Lin, K.-C.; Muthukumar, S.; Prasad, S. Flex-GO (Flexible GO) Sensor for Electrochemical Monitoring Lactate in Low-Volume Passive Perspired Human Sweat. *Talanta* **2020**, *214*, 120810. [[CrossRef](#)]
17. Wang, T.; Jing, L.-C.; Zhu, Q.; SagadevanEthiraj, A.; Tian, Y.; Zhao, H.; Yuan, X.-T.; Wen, J.-G.; Li, L.-K.; Geng, H.-Z. Fabrication of Architectural Structured Polydopamine-Functionalized Reduced GO/Carbon Nanotube/PEDOT:PSS Nanocomposites as Flexible Transparent Electrodes for OLEDs. *Appl. Surf. Sci.* **2020**, *500*, 143997. [[CrossRef](#)]
18. Ji, S.; Min, B.K.; Kim, S.K.; Myung, S.; Kang, M.; Shin, H.-S.; Song, W.; Heo, J.; Lim, J.; An, K.-S.; et al. Work Function Engineering of GO via Covalent Functionalization for Organic Field-Effect Transistors. *Appl. Surf. Sci.* **2017**, *419*, 252–258. [[CrossRef](#)]
19. Wang, C.; Zhang, Z.; Chen, B.; Gu, L.; Li, Y.; Yu, S. Design and Evaluation of Galactosylated Chitosan/GO Nanoparticles as a Drug Delivery System. *J. Colloid Interface Sci.* **2018**, *516*, 332–341. [[CrossRef](#)]
20. Berrio, M.E.; Oñate, A.; Salas, A.; Fernández, K.; Meléndrez, M.F. Synthesis and Applications of GO Aerogels in Bone Tissue Regeneration: A Review. *Mater. Today Chem.* **2021**, *20*, 100422. [[CrossRef](#)]
21. Wang, Y.; Pan, C.; Chu, W.; Vipin, A.; Sun, L. Environmental Remediation Applications of Carbon Nanotubes and GO: Adsorption and Catalysis. *Nanomaterials* **2019**, *9*, 439. [[CrossRef](#)] [[PubMed](#)]
22. Wu, Z.; Huang, W.; Shan, X.; Li, Z. Preparation of a Porous GO/Alkali Lignin Aerogel Composite and Its Adsorption Properties for Methylene Blue. *Int. J. Biol. Macromol.* **2020**, *143*, 325–333. [[CrossRef](#)] [[PubMed](#)]
23. Ain, Q.-U.; Farooq, M.U.; Jalees, M.I. Application of Magnetic GO for Water Purification: Heavy Metals Removal and Disinfection. *J. Water Process Eng.* **2020**, *33*, 101044. [[CrossRef](#)]
24. Velusamy, S.; Roy, A.; Sundaram, S.; Kumar Mallick, T. A Review on Heavy Metal Ions and Containing Dyes Removal Through GO-Based Adsorption Strategies for Textile Wastewater Treatment. *Chem. Rec.* **2021**, *21*, 1570–1610. [[CrossRef](#)] [[PubMed](#)]
25. Bhattacharjee, T.; Rahman, S.; Deka, D.; Purkait, M.K.; Chowdhury, D.; Majumdar, G. Synthesis and Characterization of Exfoliated Beta-Cyclodextrin Functionalized GO for Adsorptive Removal of Atenolol. *Mater. Chem. Phys.* **2022**, *288*, 126413. [[CrossRef](#)]
26. Delhiraja, K.; Vellingiri, K.; Boukhvalov, D.W.; Philip, L. Development of Highly Water Stable GO-Based Composites for the Removal of Pharmaceuticals and Personal Care Products. *Ind. Eng. Chem. Res.* **2019**, *58*, 2899–2913. [[CrossRef](#)]
27. Ouyang, J.; Zhou, L.; Liu, Z.; Heng, J.Y.Y.; Chen, W. Biomass-Derived Activated Carbons for the Removal of Pharmaceutical Mircopollutants from Wastewater: A Review. *Sep. Purif. Technol.* **2020**, *253*, 117536. [[CrossRef](#)]
28. Thiebault, T. Raw and Modified Clays and Clay Minerals for the Removal of Pharmaceutical Products from Aqueous Solutions: State of the Art and Future Perspectives. *Crit. Rev. Environ. Sci. Technol.* **2020**, *50*, 1451–1514. [[CrossRef](#)]
29. Emam, H.E.; El-Shahat, M.; Abdelhameed, R.M. Observable Removal of Pharmaceutical Residues by Highly Porous Photoactive Cellulose Acetate@MIL-MOF Film. *J. Hazard. Mater.* **2021**, *414*, 125509. [[CrossRef](#)]
30. HooriabadSaboore, F.; Nasirpour, N.; Shahsavari, S.; Kazemian, H. The Effectiveness of MOFs for the Removal of Pharmaceuticals from Aquatic Environments: A Review Focused on Antibiotics Removal. *Chem.-Asian J.* **2022**, *17*, e202101105. [[CrossRef](#)]
31. Ghasemi, M.; Khedri, M.; Didandeh, M.; Taheri, M.; Ghasemy, E.; Maleki, R.; Shon, H.K.; Razmjou, A. Removal of Pharmaceutical Pollutants from Wastewater Using 2D Covalent Organic Frameworks (COFs): An In Silico Engineering Study. *Ind. Eng. Chem. Res.* **2022**, *61*, 8809–8820. [[CrossRef](#)]
32. Karimi-Maleh, H.; Ayati, A.; Davoodi, R.; Tanhaei, B.; Karimi, F.; Malekmohammadi, S.; Orooji, Y.; Fu, L.; Sillanpää, M. Recent Advances in Using of Chitosan-Based Adsorbents for Removal of Pharmaceutical Contaminants: A Review. *J. Clean. Prod.* **2021**, *291*, 125880. [[CrossRef](#)]
33. Kebede, T.G.; Dube, S.; Nindi, M.M. Biopolymer Electrospun Nanofibres for the Adsorption of Pharmaceuticals from Water Systems. *J. Environ. Chem. Eng.* **2019**, *7*, 103330. [[CrossRef](#)]
34. Januário, E.F.D.; Fachina, Y.J.; Wernke, G.; Demiti, G.M.M.; Beltran, L.B.; Bergamasco, R.; Vieira, A.M.S. Application of Activated Carbon Functionalized with GO for Efficient Removal of COVID-19 Treatment-Related Pharmaceuticals from Water. *Chemosphere* **2022**, *289*, 133213. [[CrossRef](#)] [[PubMed](#)]
35. Mahmoodi, H.; Fattahi, M.; Motevassel, M. GO–Chitosan Hydrogel for Adsorptive Removal of Diclofenac from Aqueous Solution: Preparation, Characterization, Kinetic and Thermodynamic Modelling. *RSC Adv.* **2021**, *11*, 36289–36304. [[CrossRef](#)]
36. Azizian, S. Kinetic Models of Sorption: A Theoretical Analysis. *J. Colloid Interface Sci.* **2004**, *276*, 47–52. [[CrossRef](#)]
37. Weber, W.J.; Morris, J.C. Kinetics of Adsorption on Carbon from Solution. *J. Sanit. Eng. Div.* **1963**, *89*, 31–59. [[CrossRef](#)]
38. Murcia-Salvador, A.; Pellicer, J.A.; Rodríguez-López, M.I.; Gómez-López, V.M.; Núñez-Delgado, E.; Gabaldón, J.A. Egg By-Products as a Tool to Remove Direct Blue 78 Dye from Wastewater: Kinetic, Equilibrium Modeling, Thermodynamics and Desorption Properties. *Materials* **2020**, *13*, 1262. [[CrossRef](#)]
39. Nethaji, S.; Sivasamy, A.; Mandal, A.B. Adsorption Isotherms, Kinetics and Mechanism for the Adsorption of Cationic and Anionic Dyes onto Carbonaceous Particles Prepared from Juglans Regia Shell Biomass. *Int. J. Environ. Sci. Technol.* **2013**, *10*, 231–242. [[CrossRef](#)]
40. Johra, F.T.; Lee, J.-W.; Jung, W.-G. Facile and Safe Graphene Preparation on Solution Based Platform. *J. Ind. Eng. Chem.* **2014**, *20*, 2883–2887. [[CrossRef](#)]

41. Abebe, B.; Murthy, H.C.A.; Amare, E. Summary on Adsorption and Photocatalysis for Pollutant Remediation: Mini Review. *J. Encapsulation Adsorpt. Sci.* **2018**, *08*, 225–255. [[CrossRef](#)]
42. Farghali, A.A.; Bahgat, M.; El Rouby, W.M.A.; Khedr, M.H. Preparation, Decoration and Characterization of Graphene Sheets for Methyl Green Adsorption. *J. Alloys Compd.* **2013**, *555*, 193–200. [[CrossRef](#)]
43. Pholosi, A.; Naidoo, E.B.; Ofomaja, A.E. Intraparticle Diffusion of Cr(VI) through Biomass and Magnetite Coated Biomass: A Comparative Kinetic and Diffusion Study. *South Afr. J. Chem. Eng.* **2020**, *32*, 39–55. [[CrossRef](#)]
44. Falahian, Z.; Torki, F.; Faghihian, H. Synthesis and Application of Polypyrrole/Fe₃O₄ Nanosize Magnetic Adsorbent for Efficient Separation of Hg²⁺ from Aqueous Solution. *Glob. Chall.* **2018**, *2*, 1700078. [[CrossRef](#)]
45. Kyzas, G.Z.; Koltsakidou, A.; Nanaki, S.G.; Bikiaris, D.N.; Lambropoulou, D.A. Removal of Beta-Blockers from Aqueous Media by Adsorption onto GO. *Sci. Total Environ.* **2015**, *537*, 411–420. [[CrossRef](#)]

Disclaimer/Publisher's Note: The statements, opinions and data contained in all publications are solely those of the individual author(s) and contributor(s) and not of MDPI and/or the editor(s). MDPI and/or the editor(s) disclaim responsibility for any injury to people or property resulting from any ideas, methods, instructions or products referred to in the content.